# 8

# Optimization in Physiological Control

## 8.1 OPTIMIZATION IN SYSTEMS WITH NEGATIVE FEEDBACK

Consider the linear, negative-feedback control system shown in Figure 8.1a. Suppose our task is to select a suitable controller transfer function, $G_c(s)$, that would enable the control system to minimize the effects of different types of disturbances, $\delta$, on the steady-state system output, $y(t \to \infty)$. From simple analysis, we find that

$$\Delta Y(s) = \frac{G_p(s)}{1 + G_c(s)G_p(s)}\,\delta(s) \tag{8.1}$$

Then, as was discussed for the case of the steady-state error in Section 4.5.3, the steady-state response to the disturbance can be deduced from

$$\Delta y(t \to \infty) = \lim_{s \to 0} s\,\Delta Y(s) = \lim_{s \to 0}\left(\frac{sG_p(s)}{1 + G_c(s)G_p(s)}\,\delta(s)\right) \tag{8.2}$$

We first consider the situation where $G_c(s)$ takes the form of a proportional gain, $K$. Then, the steady-state response to a unit step disturbance can be deduced by setting $\delta(s) = 1/s$ and evaluating the right-hand side of Equation (8.2):

$$\Delta y(t \to \infty) = \lim_{s \to 0}\left(\frac{G_p(s)}{1 + KG_p(s)}\right) = \frac{G_{pss}}{1 + KG_{pss}} \tag{8.3}$$

Thus, in order for the system to be minimally perturbed by the step disturbance, it would be necessary to set the proportional controller gain $K$ to as large a value as possible. However, raising this gain would also predispose the system to instability, as we discussed in Chapter 6. Now, consider an alternative: Suppose our choice for $G_c(s)$ is an integral controller, $K/s$.

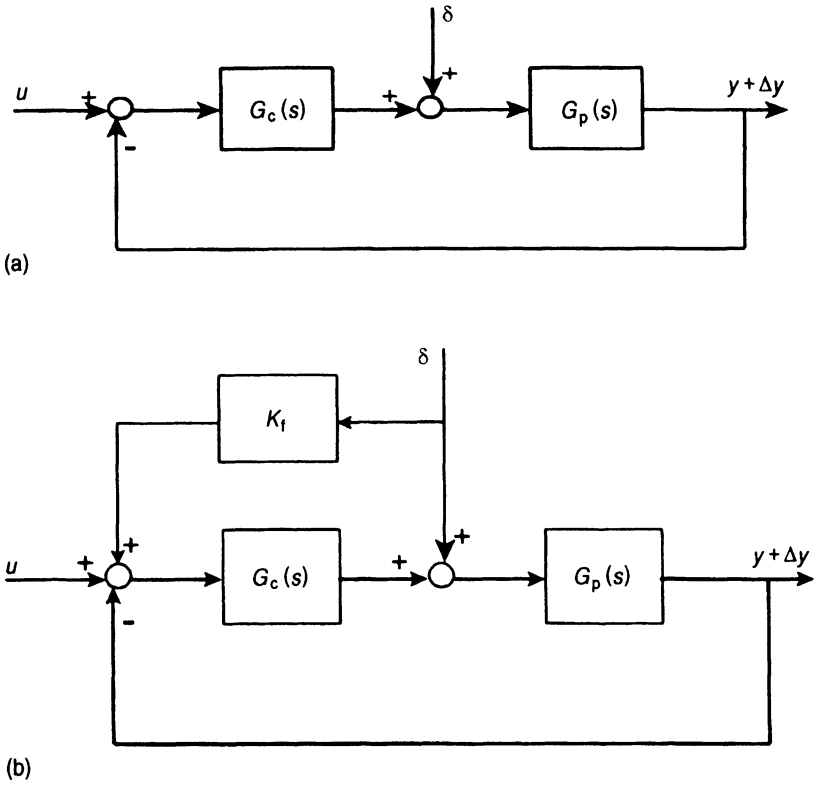


**Figure 8.1** (a) Control system utilizing only feedback. (b) Feedback control system with added feedforward element to cancel out effect of plant disturbance.

If we repeated the calculations performed above, we would obtain the following results. The closed-loop response to a unit step perturbation would be

$$\Delta y(t \to \infty) = \lim_{s \to 0} \left( \frac{G_p(s)}{1 + \frac{K}{s} G_p(s)} \right) = 0 \tag{8.4}$$

Thus, in this case, the steady-state response to the step perturbation is zero. However, the incorporation of the integral controller will slow the transition to the steady state. Therefore, in terms of minimizing the steady-state response of the system to step disturbances, we would choose an integral controller for $G_c(s)$. However, if the disturbance were to take the form of a ramp, $\delta(s) = 1/s^2$, the integral controller would result in a system response given by

$$\Delta y(t \to \infty) = \lim_{s \to 0} \left( \frac{sG_p(s)}{1 + \frac{K}{s} G_p(s)} \frac{1}{s^2} \right) = \frac{G_{pss}}{KG_{pss}} = \frac{1}{K} \tag{8.5}$$

Here, although the steady-state response of the system with integral controller to impulsive and step disturbances is zero, ramplike disturbances would still affect the system response, unless the gain of the controller were to be increased to infinity.

An alternative scheme for buffering the closed-loop response to external disturbances is shown in Figure 8.1b. Here we have added an element that senses the disturbance and produces a proportional output that is "fed forward" into the closed-loop system. This

component is known as a *feed-forward* element. The system response to the disturbance is now given by

$$\Delta Y(s) = \frac{G_p(s)(1 + K_f G_c(s))}{1 + G_c(s)G_p(s)}\,\delta(s) \tag{8.6}$$

Again, if $G_c(s)$ is a proportional controller with gain $K$, and $\delta(s)$ takes the form of a unit step, then the steady-state change in the output becomes

$$\Delta y(t \to \infty) = \lim_{s\to 0} s\,\Delta Y(s) = \lim_{s\to 0}\left(\frac{sG_p(s)(1 + K_f K)}{1 + KG_p(s)}\,\frac{1}{s}\right) = \frac{G_{pss}(1 + K_f K)}{1 + KG_{pss}} \tag{8.7}$$

The steady-state response to the disturbance can be made to become zero if the feedforward gain $K_f$ is set equal to the negative inverse of the controller gain, i.e.,

$$K_f = \frac{-1}{K} \tag{8.8}$$

The discussion above illustrates the kind of considerations that a designer of an engineering control system would make if the sole purpose of the design were to eliminate the steady-state influences of external disturbances to the system. However, it is also clear that these considerations represent an oversimplification of what would have be taken into account in the design of a "real" control system. In the examples discussed, we used as the measure of "performance" the steady-state system response to an external disturbance: the "better" system would be the one in which the disturbance produced the smaller steady-state change in output. Instead of this criterion, we could have based our performance measure on the complete (i.e., transient+steady state) response to the disturbance. A different performance measure would be likely to have led us to a different conclusion as to which controller design is the most meritorious. Thus, the *optimal* solution is not necessarily a unique one and depends heavily on the *criterion* used to measure performance.

These considerations inevitably lead to the question of whether "optimality" may be found in physiological control systems. It would seem reasonable to hypothesize that evolutionary changes and natural selection have endowed the organisms of today with the more robust of designs. However, it is unclear whether we would expect to find optimal solutions at all levels of organization—subcellular, cellular, tissue, organ, whole-body—and whether such optimal solutions are adhered to at all times. Furthermore, what would be the performance criteria involved in the optimization? The more complex systems tend to show greater redundancy in structure, which provides for greater versatility in function. As a consequence, there might be a "price" that has to be paid in the optimality of certain functions relative to others. Although the concept of biological optimization has been explored for several decades, there remains no clear consensus whether it is a general principle that is embedded in the design of all physiological systems. The problem has been that it is extremely difficult to "prove" the existence of an optimal design, given the considerable variability that exists across individual subjects. Nevertheless, the idea of optimization and its application in various physiological systems are interesting of themselves and warrant some attention. Optimization principles become particularly useful, however, in the design of "smart" devices that are to be used for artificial control or replacement of physiological organ systems or some of their components. In the rest of this chapter, we will explore some of the models that have proposed the minimization of power as the basis on which respiratory and cardiac flow patterns are optimally controlled. This survey is also

intended to provide the reader with a sense of the methodology employed to deduce the optimal solutions. As well, we will introduce the notion of adaptive control as a means of optimization and illustrate, in a given example, the application of this principle to the problem of on-line closed-loop physiological control.

## 8.2 SINGLE-PARAMETER OPTIMIZATION: CONTROL OF RESPIRATORY FREQUENCY

The notion that the respiratory frequency may be chosen by the controller on the basis that it will minimize the work rate of breathing was first proposed by Rohrer (1925). Subsequently, Otis, Fenn, and Rahn (1950) conducted a quantitative analysis to determine the optimal frequency that would be predicted through such a hypothesis. The Otis model assumes that the expiratory phase is completely passive and, therefore, that the work done in each breath occurs only in inspiration. The pattern of airflow is assumed sinusoidal, so that

$$\dot{V} = \dot{V}_{\max} \sin 2\pi f t \tag{8.9a}$$

Since the integral of airflow over the inspiratory duration equals the tidal volume, $V_T$, we have

$$V_T = \int_0^{1/2f} \dot{V}_{\max} \sin 2\pi f t \, dt = \frac{\dot{V}_{\max}}{\pi f} \tag{8.10}$$

The work expended per breath is given by

$$W = \int_0^{V_T} p \, dV \tag{8.11}$$

where $p$, the pressure developed by the inspiratory muscles at any given instant during inspiration, is given by

$$p = KV + K'\dot{V} + K''\dot{V}^2 \tag{8.12}$$

In Equation (8.12), the first term on the right-hand side represents that portion of the inspiratory muscle pressure that goes to overcoming the elastic forces that resist the expansion in lung volume, $V$, that occurs above the relaxation lung volume (or functional residual capacity). The constant $K$, therefore, represents lung stiffness, and its inverse would be equal to lung compliance. The second and third terms represent the components of pressure required to overcome the resistive forces as the air is drawn through the large and small airways. The coefficient of the second term, $K'$, is simply the linear viscous resistance to the flow through the airways as well as the nonelastic deformation of lung tissue. The third coefficient, $K''$, multiplied by the square of the airflow represents the nonlinear part of the resistance due to turbulence in airflow through the larger airways as well as the nonlinearity in lung deformation. Substituting Equation (8.12) into Equation (8.11) yields

$$W = \int_0^{V_T} (KV + K'\dot{V} + K''\dot{V}^2) \, dV \tag{8.13a}$$

However, note that since $\dot{V} \equiv dV/dt$, Equation (8.9a) can be rewritten as

$$dV = \dot{V}_{\max} \sin 2\pi f t \, dt \tag{8.9b}$$

Then, using Equation (8.10) to replace $\dot{V}_{\max}$, we obtain:

$$dV = \pi f V_T \sin 2\pi f t \, dt \tag{8.9c}$$

Using Equation (8.9c), we change the integration variable from volume ($V$) to time ($t$) in the second and third terms of Equation (8.13a). This leads to

$$W = \int_0^{V_T} KV\,dV + \pi f V_T \int_0^{1/2f} K'\dot{V}\sin 2\pi f t\,dt + \pi f V_T \int_0^{1/2f} K''\dot{V}^2 \sin 2\pi f t\,dt \quad (8.13b)$$

Then, substituting Equation (8.9a) into Equation (8.13b) and evaluating the resulting definite integrals, we obtain

$$W = \tfrac{1}{2}KV_T^2 + \tfrac{1}{4}K'\pi^2 f V_T^2 + \tfrac{2}{3}K''\pi^2 f^2 V_T^3 \quad (8.14)$$

Since this is the work expended per breath, the total inspiratory work per unit time can be derived by multiplying $W$ by the respiratory frequency $f$. Thus, the work rate is given by

$$\dot{W} = \tfrac{1}{2}Kf V_T^2 + \tfrac{1}{4}K'\pi^2 f^2 V_T^2 + \tfrac{2}{3}K''\pi^2 f^3 V_T^3 \quad (8.15)$$

Equation (8.15) highlights the fact that the work rate is a function of both respiratory frequency and tidal volume. However, the relationship between $f$ and $V_T$ is constrained by their having to satisfy the requirement of maintaining alveolar ventilation ($\dot{V}_A$), and thus gas exchange, at a constant level. Since

$$\dot{V}_A = f(V_T - V_D) \quad (8.16)$$

where $V_D$ represents the volume of the non-gas-exchanging dead space, we can substitute Equation (8.16) into Equation (8.15) to eliminate $V_T$ and to obtain

$$\dot{W} = \frac{1}{2}Kf\left(\frac{\dot{V}_A}{f} + V_D\right)^2 + \frac{1}{4}K'\pi^2(\dot{V}_A + fV_D)^2 + \frac{2}{3}K''\pi^2(\dot{V}_A + fV_D)^3 \quad (8.17)$$

It may be noted from Equation (8.17) that, for given $\dot{V}_A$ and $V_D$, the resistive contributions (second and third terms on the right-hand side) to work rate increase with frequency, whereas, as frequency increases, the elastic contribution (first term) decreases. To find the "optimal" frequency that minimizes work rate, we differentiate Equation (8.17) with respect to frequency and set the result equal to zero. This yields the following fourth-order polynomial expression in $f$:

$$2K''\pi^2 V_D^2 f^4 + \pi^2\left(\frac{1}{2}K'V_D^2 + 4K''\dot{V}_A V_D\right)f^3 + \left(\frac{KV_D^2}{2} + \frac{1}{2}K'\pi^2\dot{V}_A V_D + 2K''\pi^2\dot{V}_A^2\right)f^2 - K\dot{V}_A^2 = 0 \quad (8.18)$$

The optimal respiratory frequency, $f_{opt}$, for a given set of parameter values ($\dot{V}_A$, $V_D$, $K$, $K'$ and $K''$) can be deduced by solving Equation (8.18).

The values of the lung mechanics parameters measured in three normal subjects by Otis and colleagues were $K = 8.5$ cm $H_2O$ $L^{-1}$, $K' = 0.0583$ cm $H_2O$ min $L^{-1}$, and $K'' = 4.167 \times 10^{-4}$ cm $H_2O$ $min^2$ $L^{-2}$. If we assume $\dot{V}_A$ and $V_D$ to take on typical values for a resting subject, i.e., 6 L $min^{-1}$ and 0.2 L, respectively, the dependence of work rate and its three components on respiratory frequency may be found from Equation (8.17) to take the form shown in Figure 8.2. Note that the work-rates displayed have been expressed in units of calories per minute. The model predicts that work rate is minimized at the respiratory frequency of 14 breaths $min^{-1}$. This optimal frequency is determined primarily by the elastic and linear resistive components of work-rate; the effect of the nonlinear resistance term is very small over the range of frequencies shown. A subsequent model by Mead (1960), using average muscle force as the criterion for optimization, found the optimal frequency to be at

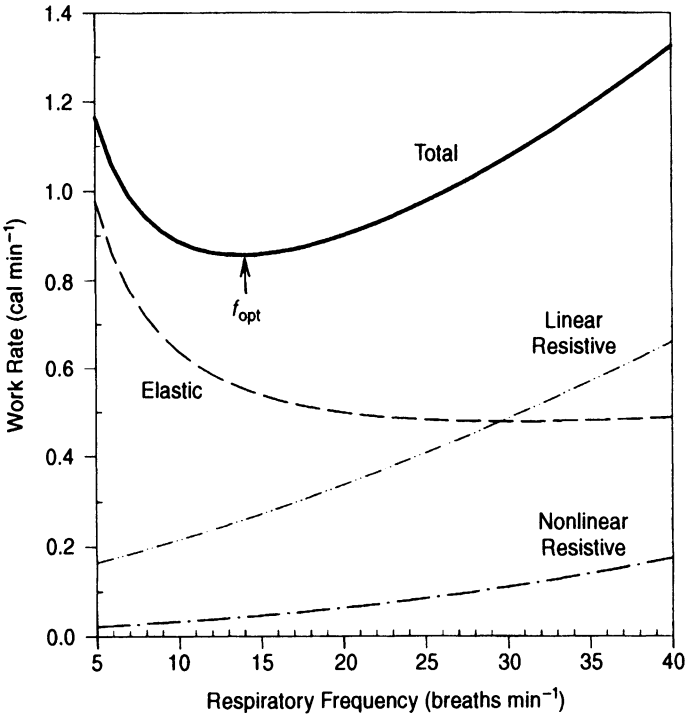


**Figure 8.2** The work-rate of breathing and its components as predicted by the Otis model. Minimization occurs at 14 breaths $min^{-1}$ ($=f_{opt}$).

the somewhat higher value of 23 breaths $min^{-1}$. Both predictions fall within the normal range of breathing frequencies observed in resting humans.

## 8.3 CONSTRAINED OPTIMIZATION: AIRFLOW PATTERN REGULATION

### 8.3.1 Lagrange Multiplier Method

In the Otis model, the somewhat restrictive assumption of a sinusoidal airflow pattern was made in order to simplify the mathematics of the problem. Since breathing patterns are generally not sinusoidal, one can take a more realistic approach by relaxing this requirement and posing the question: Is there an optimal combination of frequency and respiratory airflow pattern that minimizes the work rate of breathing? The inclusion of more unknown parameters (i.e., those characterizing airflow pattern) clearly adds greater complexity to the original problem. The approach adopted by Yamashiro and Grodins (1971) to solve this more complicated problem involved the introduction of an additional unknown parameter known as the *Lagrange multiplier*. This method of solution involves the following steps. Suppose the criterion to be optimized is $J(t, \theta_1, \theta_2, \ldots, \theta_p)$, where $\theta_i$ $(i = 1, \ldots, p)$ represent the parameters that have to be adjusted to produce the optimal value of $J$. At the same time, however, the following equality constraint must also be satisfied:

$$F(\theta_1, \theta_2, \ldots, \theta_p) = \gamma \tag{8.19}$$

where $F(\cdot)$ represents some function of the parameters and $\gamma$ is a constant. Then, a necessary condition for the required extremum is

$$\frac{\partial H}{\partial \theta_1} = \frac{\partial H}{\partial \theta_2} = \cdots = \frac{\partial H}{\partial \theta_p} = 0 \tag{8.20}$$

where the Hamiltonian, $H$, is defined as

$$H = J + \lambda F \tag{8.21}$$

and $\lambda$ is the unknown Lagrange multiplier, which needs to be determined along with the parameters $\theta_i$ $(i = 1, \ldots, p)$ by simultaneous solution of the system of equations represented by Equations (8.19) and (8.20).

### 8.3.2 Optimal Control of Airflow Pattern

In the problem at hand, the criterion to be minimized, the work-rate of breathing, is given by

$$\dot{W} = f \int_0^{V_T} P \, dV = f \int_0^{V_T} (KV + K'\dot{V}) \, dV \tag{8.22}$$

As in the Otis model, Equation (8.22) assumes that expiration is passive; however, since the contribution from nonlinear resistive contribution is relatively small, this is omitted here. In addition, the airflow pattern is periodic and the inspiratory duration is the same as the expiratory duration. Since the airflow pattern is periodic, $\dot{V}$ can be expressed in the form of a Fourier series, i.e., an infinite number of sinusoidal components:

$$\dot{V} = \sum_{i=1}^{\infty} a_i \sin 2\pi i f t \tag{8.23}$$

Using the fact that $\dot{V} = dV/dt$ and substituting Equation (8.23) into Equation (8.22), we obtain

$$\begin{aligned} \dot{W} &= \tfrac{1}{2} K f V_T^2 + K' f \int_0^{1/2f} \dot{V} \sum_{i=1}^{\infty} a_i \sin 2\pi i f t \, dt \\ &= \tfrac{1}{2} K f V_T^2 + K' f \int_0^{1/2f} \sum_{i=1}^{\infty} \sum_{k=1}^{\infty} a_i a_k \sin 2\pi i f t \sin 2\pi k f t \, dt \end{aligned} \tag{8.24a}$$

The orthogonality property of sinusoids can be used to simplify the last term in Equation (8.24a):

$$\int_0^{1/2f} \sin 2\pi i f t \sin 2\pi k f t \, dt = \begin{cases} 0 & i \neq k \\ \dfrac{1}{4f} & i = k \end{cases} \tag{8.25}$$

Thus, using Equation (8.25) in Equation (8.24a) yields the result:

$$\dot{W} = \frac{K f V_T^2}{2} + \frac{K'}{4} \sum_{i=1}^{\infty} a_i^2 \tag{8.24b}$$

$V_T$ can also be expressed as a function of the dead space, $V_D$, and alveolar ventilation, $\dot{V}_A$:

$$V_T = V_D + \frac{\dot{V}_A}{f} \tag{8.26}$$

Substituting this into Equation (8.24b), we have

$$\dot{W} = \frac{Kf}{2}\left(V_D + \frac{\dot{V}_A}{f}\right)^2 + \frac{K'}{4}\sum_{i=1}^{\infty} a_i^2 \tag{8.24c}$$

Since $V_T$ is a function of the airflow pattern,

$$V_T = \int_0^{1/2f} \sum_{i=1}^{\infty} a_i \sin 2\pi i f t \, dt = \sum_{i=1}^{\infty} \frac{a_{2i-1}}{(2i-1)\pi f} \tag{8.27}$$

The constraint that alveolar ventilation must remain constant can also be written

$$\dot{V}_A - \frac{1}{\pi}\sum_{i=1}^{\infty} \frac{a_{2i-1}}{2i-1} + fV_D = 0 \tag{8.28}$$

Thus, we can now restate the problem in a way in which the Lagrange multiplier method can be applied. We need to minimize the work rate in Equation (8.24c), subject to the constraint in Equation (8.28). To apply the Lagrange multiplier technique, we first form the Hamiltonian, which in this case is given by

$$H(f, a_1, a_2, \ldots) = \frac{Kf}{2}\left(V_D + \frac{\dot{V}_A}{f}\right)^2 + \frac{K'}{4}\sum_{i=1}^{\infty} a_i^2 + \lambda\left[\dot{V}_A - \frac{1}{\pi}\sum_{i=1}^{\infty} \frac{a_{2i-1}}{2i-1} + fV_D\right] \tag{8.29}$$

Next, we differentiate $H$ with respect to each of these parameters and set the result in each case equal to zero:

$$\frac{\partial H}{\partial f} = \frac{K}{2}\left(V_D^2 - \frac{\dot{V}_A^2}{f^2}\right) + \lambda V_D = 0 \tag{8.30}$$

and

$$\frac{\partial H}{\partial a_i} = \frac{K'a_i}{2} = 0 \qquad \text{for even values of } i \tag{8.31a}$$

$$= \frac{K'a_i}{2} - \frac{\lambda}{\pi i} = 0 \qquad \text{for odd values of } i \tag{8.31b}$$

The optimal parameter values are deduced by simultaneous solution of Equations (8.28), (8.30), and (8.31). Note from Equation (8.31a) that all the Fourier coefficients that represent even harmonics of the fundamental frequency $f$ (i.e., $a_{2m}$) equal zero. Thus, from Equation (8.31b), we have

$$a_{2m-1} = \frac{2\lambda}{K'\pi(2m-1)} \tag{8.32}$$

Substituting this result into Equation (8.28) yields

$$\frac{2\lambda}{K'\pi^2}\sum_{i=1}^{\infty} \frac{1}{(2i-1)^2} = \dot{V}_A + fV_D \tag{8.33}$$

However, a useful expansion result that helps to greatly simplify Equation (8.33) is

$$\sum_{i=1}^{\infty} \frac{1}{(2i-1)^2} = \frac{\pi^2}{8} \tag{8.34}$$

Substituting Equation (8.34) into Equation (8.33) gives the final result for $\lambda$:

$$\lambda = 4K'(\dot{V}_A + fV_D) \tag{8.35}$$

The optimal frequency, $f_{opt}$, is deduced by substituting Equation (8.35) into Equation (8.30):

$$f_{opt} = \frac{K}{16K'}\left(\sqrt{1 + \frac{32K'\dot{V}_A}{KV_D}} - 1\right) \tag{8.36}$$

To obtain the optimal airflow pattern coefficients, we employ Equation (8.35) in Equation (8.32):

$$a_{2i-1} = \frac{8}{\pi(2i-1)}(\dot{V}_A + fV_D) \tag{8.37}$$

The optimal airflow pattern is thus characterized by the Fourier series expansion:

$$\dot{V} = 2(\dot{V}_A + fV_D)\left(\frac{4}{\pi}\sin 2\pi ft + \frac{4}{3\pi}\sin 6\pi ft + \frac{4}{5\pi}\sin 10\pi ft + \cdots\right) \tag{8.38}$$

which corresponds to a square wave of amplitude $2(\dot{V}_A + fV_D)$. One should recall, however, that we had assumed expiratory flow to be completely passive. Therefore, the above pattern applies only during inspiration. During expiration, the inspiratory muscle pressure is zero, and thus

$$P = KV + K'\frac{dV}{dt} = 0 \tag{8.39}$$

Integrating Equation (8.39) with respect to time ($1/2f_{opt} < t < 1/f_{opt}$), with the initial condition (at $t = 1/2f_{opt}$ or end inspiration) of $V = V_T$, we get

$$V(t) = V_T e^{-K(t-1/2f)/K'} \qquad \frac{1}{2f} \le t < \frac{1}{f} \tag{8.40}$$

Finally, differentiating $V(t)$ with respect to time, we obtain the airflow time-course during expiration:

$$\dot{V} = -\frac{KV_T}{K'}e^{-K(t-1/2f)/K'} \qquad \frac{1}{2f} \le t < \frac{1}{f} \tag{8.41}$$

The complete airflow pattern of the optimal breath is shown in Figure 8.3a. Using Equation (8.24b), the work-rates of breathing corresponding to this airflow pattern at different frequencies can be computed and are displayed in Figure 8.3b. For comparison, the corresponding prediction from the Otis model is also shown. For the same lung mechanical parameter values, and for $\dot{V}_A = 6$ L min$^{-1}$ and $V_D = 0.2$ L, an optimal respiratory frequency of 16 breaths min$^{-1}$ is predicted. This is slightly higher than the optimal frequency (14 breaths min$^{-1}$) predicted by the Otis model, but falls within the range of physiological variability. However, observed inspiratory airflow patterns resemble the model prediction only during exercise or when subjects breathe through external resistances. Under such conditions, the assumption of a completely passive expiration may be violated. If expiration is assumed

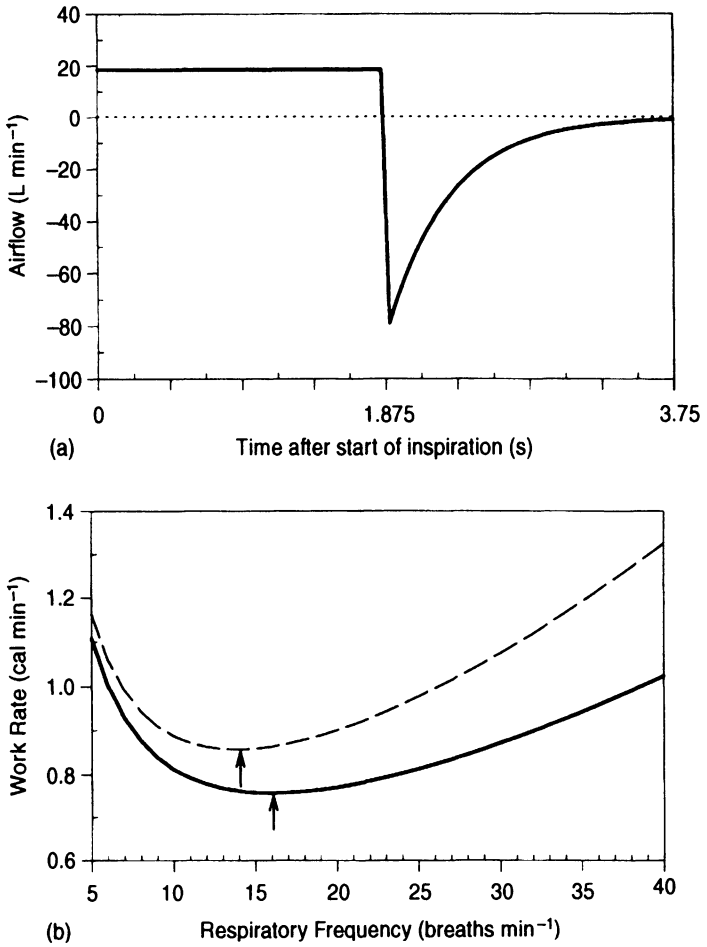


**Figure 8.3** (a) Optimal airflow pattern predicted by the Yamashiro and Grodins model for $\dot{V}_A = 6\,\text{L min}^{-1}$ and $V_D = 0.2\,\text{L}$. (b) Comparison of predicted dependence of work-rate on frequency between the Yamashiro and Grodins model (solid curve) and the Otis model (broken curve). Arrows indicate the location of the optimal frequencies.

active, the model predicts an optimal square-wave pattern of breathing (in expiration as well as inspiration); however, there is no optimal frequency. At higher rates of breathing and flows, the effects of airflow turbulence and fluid inertia may not be negligible, as was assumed here. On the other hand, Ruttimann and Yamamoto (1972) have demonstrated that inclusion of these factors does not change the optimal square-wave strategy for the regulation of airflow.

## 8.4 CONSTRAINED OPTIMIZATION: CONTROL OF AORTIC FLOW PULSE

### 8.4.1 Calculus of Variations

In situations where the criterion function to be minimized and the constraints are in the form of integral equations, the method of *calculus of variations* constitutes a useful approach.

In fact, this approach represents a generalization of the Lagrange multiplier method discussed in Section 8.3. Suppose the criterion to be optimized is of the form

$$I = \int_{t_0}^{t_1} J(t, \theta_1, \dot{\theta}_1, \theta_2, \dot{\theta}_2, \ldots, \theta_p, \dot{\theta}_p)\, dt \tag{8.42}$$

where $\theta_i(t)$; $(i = 1, 2, \ldots, p)$ are the functions that produce the optimal value of $I$. At the same time, we assume for generality that two types of equality constraints have to be satisfied. The first kind takes the form of $M$ definite integrals, each of which equals some known constant value, $\gamma_k$ $(1 \leq k \leq M)$:

$$\int_{t_0}^{t_1} F_k(t, \theta_1, \dot{\theta}_1, \theta_2, \dot{\theta}_2, \ldots, \theta_p, \dot{\theta}_p)\, dt = \gamma_k, \qquad \text{where } k = 1, \ldots, M \tag{8.43}$$

The second kind of equality constraints take the form of nonintegral type equations:

$$G_i(\theta_1, \dot{\theta}_1, \theta_2, \dot{\theta}_2, \ldots, \theta_p, \dot{\theta}_p) = 0, \qquad \text{where } i = 1, \ldots, N \tag{8.44}$$

Then, the necessary conditions for the required extremum are given by the set of Euler equations:

$$\begin{aligned} &\frac{\partial H}{\partial \theta_1} - \frac{d}{dt}\left(\frac{\partial H}{\partial \dot{\theta}_1}\right) = 0 \\ &\qquad\vdots \\ &\frac{\partial H}{\partial \theta_p} - \frac{d}{dt}\left(\frac{\partial H}{\partial \dot{\theta}_p}\right) = 0 \end{aligned} \tag{8.45}$$

where $H$, the *adjoined criterion function*, is defined as

$$H = J + \sum_{k=1}^{M} \lambda_k F_k + \sum_{i=1}^{M} \mu_i(t) G_i \tag{8.46}$$

In Equation (8.46), $\lambda_k$ $(1 \leq k \leq M)$ are unknown Lagrange multiplier constants that have to be estimated along with the other parameters. In addition to these, there are also $N$ time-dependent Lagrange multipliers, $\mu_i$ $(1 \leq i \leq N)$, that have to be determined. Thus, the unknown functions $\theta_i(t)$ $(i = 1, 2, \ldots, p)$ can be deduced along with these two sets of Lagrange multipliers through simultaneous solution of Equations (8.43), (8.44), and (8.45).

### 8.4.2 Optimal Left Ventricular Ejection Pattern

The method of calculus of variations has been applied to the problem of predicting the optimal left ventricular ejection pattern that would minimize the power expended during the cardiac cycle for a given level of cardiac output (Yamashiro et al., 1979). The electrical analog of the simple model assumed in this problem is shown in Figure 8.4. Blood from the left ventricle is ejected through the aortic valve, which has resistance $R_C$, into the systemic circulation, which has a lumped resistance and compliance of $R_P$ and $C_A$, respectively. $Q(t)$ and $q(t)$ represent the time-courses of blood flow leaving the left ventricle and entering the systemic circulation, respectively. We assume that the duration of systole is $T_S$ and the total

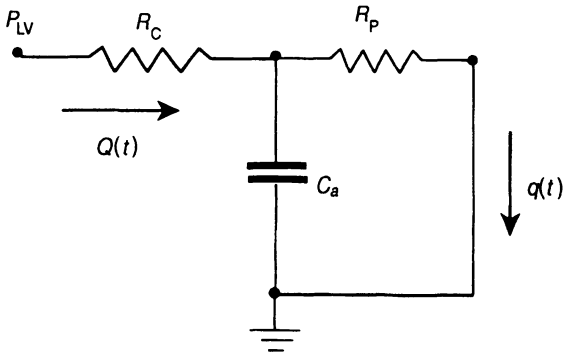


**Figure 8.4** Electrical analog of cardiovascular model used to determine the optimal aortic root flow pattern for given cardiac output. $P_{LV}$ = left ventricular pressure. Other symbols are defined in the text.

duration of the cardiac cycle is $T$. For constant cardiac output, the stroke volume, $V_S$, must also be constant, i.e.,

$$V_S = \int_0^{T_S} Q(t)\, dt = \text{constant} \tag{8.47}$$

The above equation constitutes one constraint that has to be met. A second constraint arises from the conservation of mass principle (or equivalently, Kirchhoff's law for currents entering and leaving the middle node in the electric analog in Figure 8.4):

$$Q(t) = R_P C_a \frac{dq}{dt} + q(t) \tag{8.48}$$

It is also assumed that during diastole, the aortic valve is closed, so that

$$Q(t) = 0, \qquad T_S \leq t < T \tag{8.49}$$

During this interval, the part of the original ventricular output that accumulated in the arterial capacitance in systole is discharged into the rest of the circulation. Thus, the peripheral flow, $q(t)$, during the interval $T_S \leq t < T$ is determined by the solution to Equation (8.48) with $Q(t)$ set equal to zero, i.e.:

$$q(t) = q_{T_S} e^{-(t-T_S)/R_P C_a} \tag{8.50}$$

But, at $t = T$, the value of $q(t)$ must be equal to its value at the start of the cycle. Thus,

$$q(T) = q_0 = q_{T_S} e^{-(T-T_S)/R_P C_a} \tag{8.51a}$$

or

$$q_{T_S} = q(T_S) = q_0 e^{(T-T_S)/R_P C_a} \tag{8.51b}$$

Thus, for given $T$, $T_S$, and initial condition $q_0$, $q_{T_S}$ in Equation (8.51b) provides the boundary condition that must be applied for the determination of the unique optimal solution of $q(t)$.

Similar considerations also apply to the energy balance. During systole, part of the energy expended is stored as elastic energy in the arterial capacitance. However, during diastole, all this stored energy is dissipated as continuing flow through the systemic circulation. Therefore, over the entire cardiac cycle, the total energy dissipated is given by

$$W = R_C \int_0^{T_S} Q^2(t)\, dt + R_P \int_0^{T_S} q^2(t)\, dt + R_P \int_{T_S}^{T} q^2(t)\, dt \tag{8.52}$$

However, the energy dissipated during diastole (last term of Equation (8.52)) is independent of the time-course of $Q(t)$, since Equations (8.50) and (8.51b) show that $q(t)$ during this interval is a function only of $q_0$ and the cardiovascular mechanical parameters. Thus, it is possible to simplify the problem by defining the criterion function that we wish to minimize to be

$$W_S = R_C \int_0^{T_S} Q^2(t)\, dt + R_P \int_0^{T_S} q^2(t)\, dt \tag{8.53}$$

The problem can now be restated as follows: determine the time-courses of $Q(t)$ and $q(t)$ that would minimize $W_S$ in Equation (8.53), while satisfying the constraints given by Equations (8.47) and (8.48). This can clearly be solved by applying the method of calculus of variations (Section 8.4.1). Note that Equation (8.47) takes the form of a definite integral and is therefore a constraint of the type represented by Equation (8.43). Equation (8.48), on the other hand, does not explicitly contain any integrals; thus, in this case, it is an equality constraint of the type represented by Equation (8.44). These considerations lead to the following adjoined criterion function ($H$) that provides us with the capability of taking both types of equality constraints into account:

$$\begin{aligned} H &= W_S + \lambda Q(t) + \mu(t)[Q(t) - R_P C_a \dot{q}(t) - q(t)] \\ &= R_C Q^2(t) + R_P q^2(t) + \lambda Q(t) + \mu(t)[Q(t) - R_P C_a \dot{q}(t) - q(t)] \end{aligned} \tag{8.54}$$

The corresponding Euler equations are

$$\frac{\partial H}{\partial Q} - \frac{d}{dt}\left(\frac{\partial H}{\partial \dot{Q}}\right) = 2R_C Q(t) + \lambda + \mu(t) = 0 \tag{8.55}$$

and

$$\frac{\partial H}{\partial q} - \frac{d}{dt}\left(\frac{\partial H}{\partial \dot{q}}\right) = 2R_P q(t) - \mu(t) + R_p C_a \dot{\mu}(t) = 0 \tag{8.56}$$

We use Equations (8.55) and (8.56) to eliminate $\mu(t)$ and $\dot{\mu}(t)$, yielding the following result:

$$R_P q(t) + R_C Q(t) + \frac{\lambda}{2} - R_C \tau \dot{Q}(t) = 0 \tag{8.57}$$

where we now define

$$\tau = R_P C_a \tag{8.58}$$

Equation (8.48) is used to eliminate $Q(t)$ and $\dot{Q}(t)$ from Equation (8.57), leading to the following result:

$$\ddot{q}(t) - \alpha^2 q(t) = \frac{\lambda}{2\tau^2 R_C} \tag{8.59}$$

where

$$\alpha = \frac{1}{\tau}\sqrt{\frac{R_P + R_C}{R_C}} \tag{8.60}$$

Solution of Equation (8.59) yields

$$q(t) = \left(q_0 + \frac{\lambda}{2(R_P + R_C)}\right)\cosh \alpha t + \frac{q(0)}{\alpha}\sinh \alpha t - \frac{\lambda}{2(R_P + R_C)} \tag{8.61}$$

In the above result, note that $\dot{q}(0)$ and $\lambda$ are unknown quantities that need to be determined. The former can be found by evaluating Equation (8.61) at $t = T_S$, and using Equation (8.51b) to relate $q(T_S)$ to $q_0$ and the other known quantities. This leads to the following result for the optimal $q(t)$:

$$q(t) = A_1 \cosh(\alpha t) + A_2 \sinh(\alpha t) - A_0 \tag{8.62}$$

where

$$A_0 = \frac{\lambda}{2(R_P + R_C)} \tag{8.63}$$

$$A_1 = q_0 + A_0 \tag{8.64}$$

and

$$A_2 = \frac{1}{\sinh(\alpha T_S)}\left[q_0 e^{(T-T_S)/\tau} + A_0 - A_1 \cosh(\alpha T_S)\right] \tag{8.65}$$

Using Equation (8.62), we can evaluate Equation (8.48) to obtain an expression for the optimal $Q(t)$:

$$Q(t) = (\tau\alpha A_1 + A_2)\sinh \alpha t + (\tau\alpha A_2 + A_1)\cosh \alpha t - A_0 \tag{8.66}$$

Note, however, that the expressions for optimal $q(t)$ and $Q(t)$ still contain an unknown parameter: $\lambda$. The latter can be eliminated by using the remaining constraint equation that has not been employed thus far, i.e., Equation (8.47). Therefore, in accordance with Equation (8.47), we integrate $Q(t)$ in Equation (8.66) with respect to time over the interval $t = 0$ to $t = T_S$ and equate the result to the stroke volume $V_S$. This allows us to solve for $\lambda$:

$$\lambda = \frac{2(R_C + R_P)\left(V_S - q_0 B_1 - \dfrac{B_2 B_3}{\sinh \alpha T_S}\right)}{B_1 + B_3\left(\dfrac{1 - \cosh \alpha T_S}{\sinh \alpha T_S}\right) - T_S} \tag{8.67}$$

where

$$B_1 = \tau(\cosh \alpha T_S - 1) + \frac{1}{\alpha}\sinh \alpha T_S \tag{8.68}$$

$$B_2 = q_0(e^{(T-T_S)/\tau} - \cosh \alpha T_S) \tag{8.69}$$

and

$$B_3 = \frac{1}{\alpha}(\cosh \alpha T_S - 1) + \tau \sinh \alpha T_S \tag{8.70}$$

Thus, for given $T$, $V_S$, $R_C$, $R_P$, $C_a$, and $q_0$, Equations (8.66) and (8.67) can be used to deduce the time-course of $Q(t)$ as a function of the duration of systole, $T_S$. One implicit constraint remains to be satisfied. To obtain the optimal $T_S$ and $Q(t)$, the appropriate value of $T_S$ must be selected by some search procedure so that $Q(T_S)$ becomes zero. This is illustrated in Figure 8.5. Here, $Q(T_S)$ is plotted against $T_S$ for three different levels of $R_P$. As $T_S$

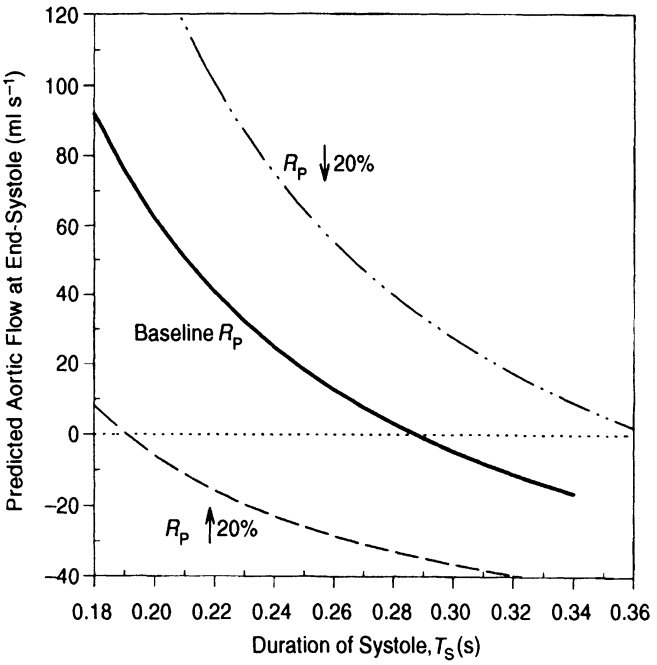


**Figure 8.5** Variation of predicted end-systolic aortic flow with duration of systole at different levels of peripheral resistance. The optimal systolic duration is the value that produces zero end-systolic aortic flow.

increases, $Q(T_S)$ decreases from positive values towards negative values. Thus, the value of $T_S$ at which $Q(T_S)$ becomes zero is the optimal value of $T_S$ that allows the systolic portion of the solution to be continuous with the diastolic portion. For baseline levels of $R_P$, optimal $T_S$ is 0.29 s. However, as $R_P$ increases, optimal $T_S$ decreases (i.e., the duration of systole becomes shorter), and vice versa.

The optimal time-courses for $Q(t)$ and $q(t)$ predicted by the model are displayed in Figures 8.6a and 8.6b, respectively. The solid curves represent the predictions made with the assumption of "nominal" parameter values for a 10 kg dog at rest. These parameter values are: $T = 0.5$ s, $q_0 = 19.16\,\text{ml s}^{-1}$, $V_S = 12$ ml, $R_C = 0.033$ mm Hg s ml$^{-1}$, $C_a = 0.178$ ml mm Hg$^{-1}$, and $R_P = 4.17$ mm Hg s mL$^{-1}$. The computation of the optimal flow patterns, as well as the initial determination of optimal $T_S$, was performed with the use of MATLAB script file "`OptLVEF.m`." As shown in Figure 8.5, the optimal duration of systole in this case is 0.29 s or 58% of the cardiac period. When $R_P$ is increased, energy expended per cardiac cycle is minimized by shortening the duration of systole and allowing the systolic aortic flow pattern to be more triangular with substantially higher flow in the early part of the cycle. With lower $R_P$, the initial high level of flow is not required and systolic duration is lengthened. These patterns resemble those observed in measurements of aortic flow pulses, except that, in the latter, aortic flow at the start of systole does not instantaneously increase to its maximum value. This prediction is due largely to the omission of fluid inertia in the model. An improved optimization model by Livnat and Yamashiro (1981), which includes blood inertia, nonlinear aortic valve resistance, and ventricular compliance, produces more realistic left ventricular pressure and flow patterns. However, the inclusion of more complexity makes it impossible to obtain a closed-form analytic solution to the problem, and a numerical method of solution is necessary.

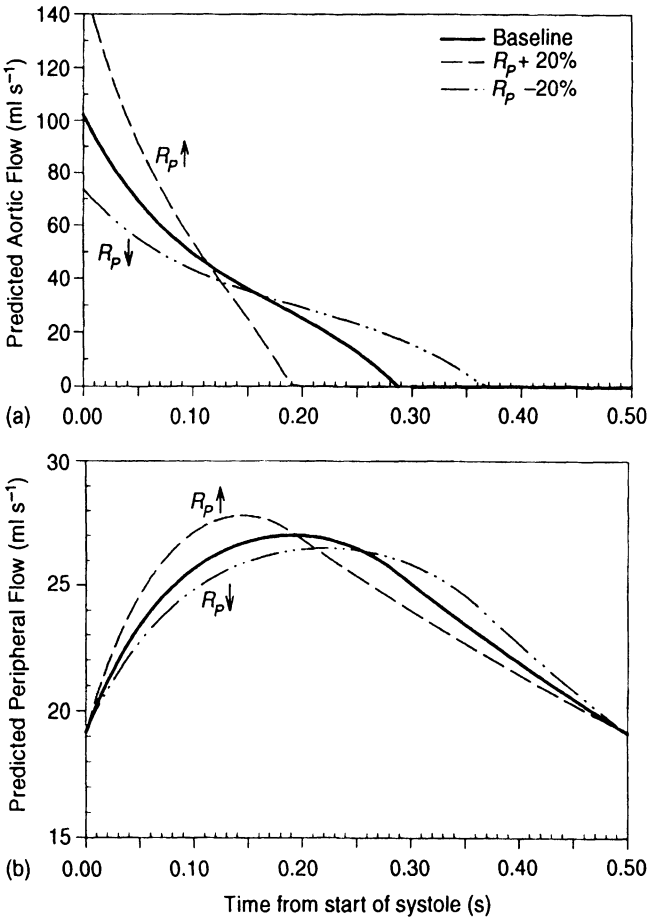


**Figure 8.6** Predicted optimal patterns of (a) aortic root flow (left ventricular output), and (b) peripheral or systemic flow at different levels of peripheral resistance.

## 8.5 ADAPTIVE CONTROL OF PHYSIOLOGICAL VARIABLES

### 8.5.1 General Considerations

Although the optimization hypothesis is teleologically attractive and has been a useful means of "explaining" specific control strategies in a number of physiological processes, whether it can be regarded as a general principle that is embedded in all biological systems at all levels of organization remains unclear at this time. On the other hand, what is clear is that all physiological systems are time-varying, i.e., their structure and governing parameters change over time. So, even if optimization has been demonstrated to exist, the next question that arises is whether this optimization is adaptive. Conversely, is the adaptive behavior of a given physiological system aimed at optimizing some measure of performance? These questions are complex and remain at the forefront of contemporary physiological (in particular, neurophysiological) research. At the same time, however, the development of medical prosthetic and assistive devices has led to substantial progress in applying the concepts of adaptive control to the problem of designing schemes for automatically

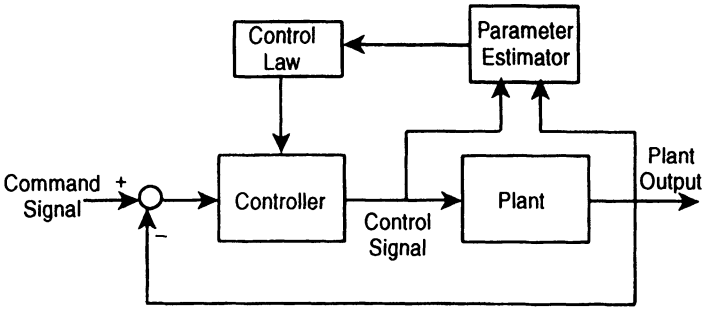


**Figure 8.7** Schematic block diagram of the general adaptive control system.

controlling various physiological variables. It is toward these kinds of adaptive control systems that we will now turn our attention, since the theory and engineering applications of such systems are well developed.

Figure 8.7 shows a block diagram for the general adaptive control system. The basic features that distinguish adaptive control from simple feedback control are the addition of a parameter estimator to determine the changes in dynamics of the unknown plant and a control law that uses an optimization algorithm to select the control signal that is optimally adjusted for the altered plant dynamics. Most adaptive control schemes require a model of the plant. Therefore, the accuracy and reliability with which this model characterizes plant dynamics are key factors that govern how well the adaptive control system will work in practice.

The two major types of adaptive controllers employed in online physiological control and closed-loop drug delivery schemes are illustrated in Figure 8.8. In the clinical setting, there is always considerable variability in plant dynamics across subjects as well as within an individual subject at different times. The *multiple model adaptive control* (MMAC) system, shown in Figure 8.8a, allows for a finite range of representations of plant states by containing a model bank. Constraints are placed on the parameters of each model employed, so that the controller responses remain reasonable and bounded. One disadvantage of this approach is that it requires significant knowledge of the plant dynamics. Another is that the controller may not be able to handle plant behavior that lies beyond the range specified in the model bank. The *model reference adaptive control* (MRAC) system, on the other hand, uses a single general model of the plant (Figure 8.8b). Thus, it can be more versatile. However, there is no guarantee of stability for the parameter estimates and for the physiological variable being controlled. Both these types of adaptive control schemes have been used in a variety of closed-loop drug delivery applications, including blood pressure control, neuromuscular blockade, and control of blood glucose level (Katona, 1982; Martin et al., 1987; Olkkola and Schwilden, 1991; Fischer et al., 1987).

### 8.5.2 Adaptive Buffering of Fluctuations in Arterial $P_{CO_2}$

A detailed consideration of adaptive control theory and its applications lies beyond the scope of this text. For this, the reader is referred to a number of excellent volumes, such as Astrom and Wittenmark (1989) and Harris and Billings (1981). However, in this section, we will illustrate an example of how this theory can be implemented in practice. The problem at hand concerns the considerable degree of breath-to-breath variability that has been observed in spontaneous ventilation. Accompanying this ventilatory variability are the corresponding

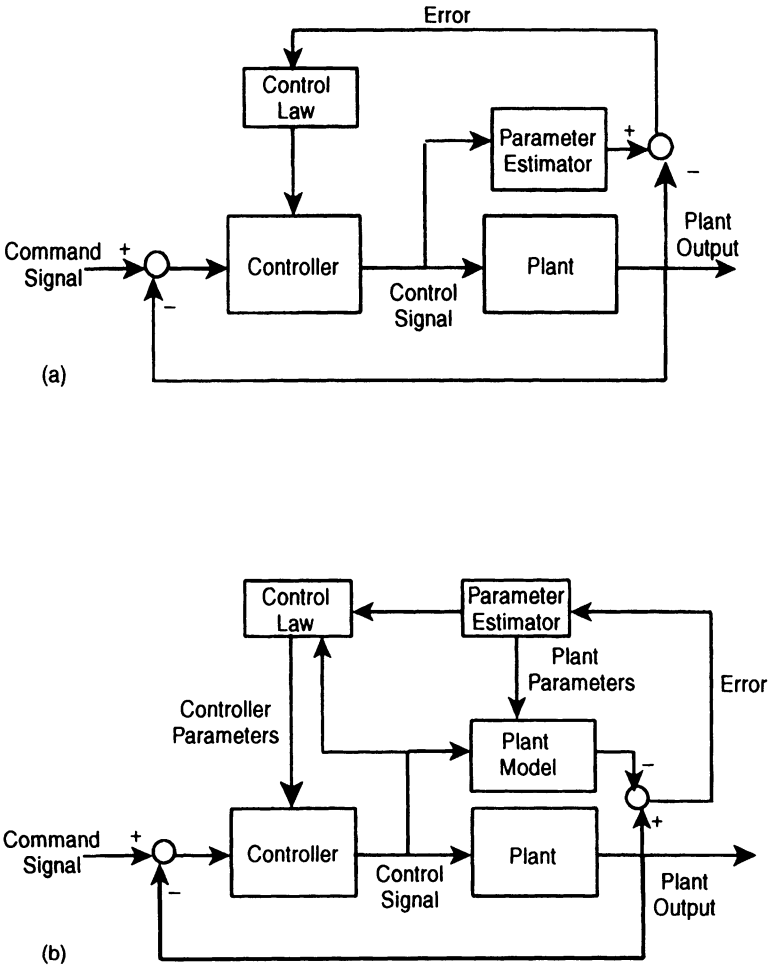


**Figure 8.8** Schematic block diagrams of (a) a multiple-model adaptive control (MMAC) system, and (b) a model reference adaptive control (MRAC) system.

fluctuations in alveolar and, therefore, arterial $P_{CO_2}$. Modarreszadeh et al. (1993) addressed the issue of buffering these fluctuations in arterial $P_{CO_2}$ in an optimal manner by changing the $CO_2$ composition of the inhaled gas ($F_{ICO_2}$) on a breath-by-breath basis. Figure 8.9 shows a block diagram of the scheme employed for achieving this goal. The bottom portion of the block diagram represents the respiratory control system. Fluctuations in arterial $P_{CO_2}$, which we assume are measured in the form of fluctuations in the end-tidal $CO_2$ fraction ($F_{ETCO_2}$), result from "ventilatory noise" entering the closed-loop system as well as changes in gas exchange dynamics in the lungs. A simple linearized model of the gas exchange process is assumed, and based on measurements of ventilation ($\dot{V}_E$) and $F_{ETCO_2}$, the plant model parameters are identified. However, since gas exchange dynamics can change with the sleep–wake state or other conditions of the subject, the estimation of plant model parameters has to be performed adaptively. At any given breath, the estimated plant model parameters are used along with existing measurements of $\dot{V}_E$ and $F_{ETCO_2}$ to predict what $F_{ICO_2}$ should be applied next to minimize the fluctuation of $F_{ETCO_2}$ in the next breath.

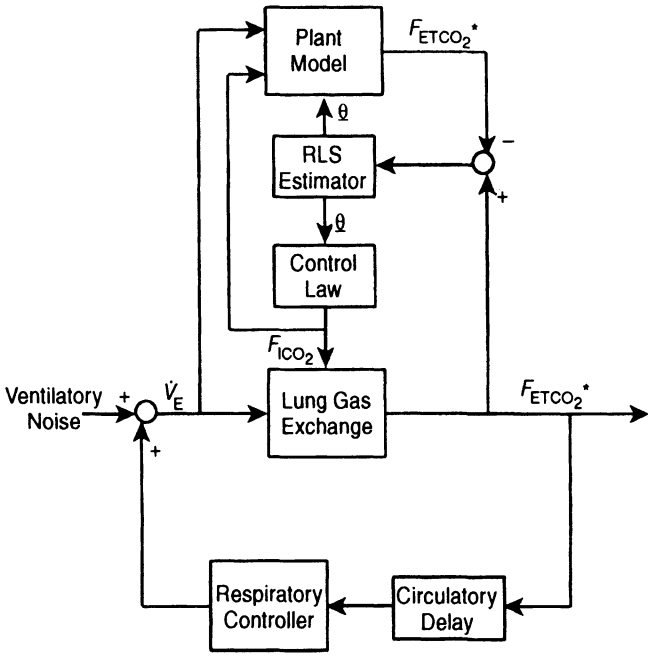


**Figure 8.9** Control scheme for adaptive buffering of spontaneous fluctuations in end-tidal $CO_2$ in humans (Modarreszadeh et al., 1993).

***8.5.2.1. Plant Model.*** Since the purpose of the scheme is to minimize the fluctuations in $F_{ETCO_2}$ about its mean level, we define the new variables $\Delta F_{ETCO_2}$, $\Delta \dot{V}_E$, and $\Delta F_{ICO_2}$ as the deviations in $F_{ETCO_2}$, $\dot{V}_E$, and $F_{ICO_2}$, respectively, about their corresponding means. Since negative $F_{ICO_2}$ cannot be realized in practice, it is assumed that the "resting" or mean level of $F_{ICO_2}$, prior to the application of adaptive control, is 2.5% and not zero (i.e., the subject is breathing a gas mixture that resembles air but contains a small amount of $CO_2$). The linearized plant model takes a form very similar to that given in Equation (7.64a) in Section 7.5.2:

$$\begin{aligned}\Delta F_{ETCO_2}(n) = a(n)\,\Delta F_{ETCO_2}(n-1) + b(n)\,\Delta \dot{V}_E(n-1) \\ + c(n)\,\Delta F_{ICO_2}(n-1) + e(n)\end{aligned} \tag{8.71}$$

Apart from the fact that $\Delta F_{ETCO_2}$ and $\Delta F_{ICO_2}$ are now used in place of $\Delta P_{ACO_2}$ and $\Delta P_{ICO_2}$, respectively, a large difference between Equation (8.71) and Equation (7.64a) is that the unknown parameters here ($a$, $b$, and $c$) are assumed to be time-varying; $n$ refers to the current breath. Thus, $\Delta F_{ETCO_2}(n-1)$ and $\Delta \dot{V}_E(n-1)$ represent the changes in $F_{ETCO_2}$ and $\dot{V}_E$ at the *previous* breath. However, the exception is with $\Delta F_{ICO_2}(n-1)$, which represents the change in $F_{ICO_2}$ of the *current* breath. This peculiar assignment of breath number is made because, in the real-time implementation of this scheme, the measurement of $F_{ICO_2}$ in the preceding inspiration is already available for use in the algorithm during the expiratory phase of the $n$th breath. By the same token, $\Delta \dot{V}_E(n-1)$ has to be used in place of $\Delta \dot{V}_E(n)$ in Equation (8.71) (note the use of $\Delta \dot{V}_E(n)$ in Equation (7.64a)), because the computation of $\Delta \dot{V}_E(n)$ requires knowledge of the tidal volume and total period of the $n$th breath, and the latter measurement is not available until the end of the expiratory phase in the current breath ($n$). Finally, $e(n)$ in

Equation (8.71) represents the error between the measured $\Delta F_{ETCO_2}$ at breath $n$ and the corresponding value predicted by using the plant model. Thus, the predicted $\Delta F_{ETCO_2}$ ($\Delta F^*_{ETCO_2}$) is given by

$$\Delta F^*_{ETCO_2}(n) = a(n)\,\Delta F_{ETCO_2}(n-1) + b(n)\,\Delta \dot{V}_E(n-1) + c(n)\,\Delta F_{ICO_2}(n-1) \tag{8.72a}$$

***8.5.2.2. Plant Model Parameter Estimation.*** The plant model parameters are estimated adaptively, so that with each new breath, the new set of measurements obtained can be used to update our knowledge about the gas exchange process. To achieve this task, one can choose among a variety of methods for adaptive estimation. For this problem, Modarreszadeh et al. (1993) selected one that has been commonly employed in physiological system identification: the *recursive least squares* (RLS) method. For other methods, the reader is referred to texts by Orfanidis (1988), Astrom and Wittenmark (1989), and Akay (1994).

In the RLS method, the criterion function to be minimized assumes the form

$$J(n) = \sum_{i=0}^{n} \lambda^{n-i} e(i)^2 \tag{8.73}$$

where $e(i)$ represents the error between observed and predicted values of $F_{ETCO_2}$, as given in Equation (8.71), and $\lambda$ is a constant factor (with values between 0 and 1). The latter, in effect, provides a means of assigning relative weights to more recent versus more remote events. For instance, if $\lambda$ is given a value close to zero, then $J(n)$ will be determined predominantly by $e(n)$ and virtually nothing else. At the other extreme, when $\lambda$ is close to unity, $J(n)$ will be essentially equal to the sum of squares of the residuals for the current and past $n$ breaths. For this reason, $\lambda$ is often referred to as the *forgetting factor.*

Since the estimation involves three parameters, we can recast Equation (8.72a) in the form of a vector equation:

$$\Delta F^*_{ETCO_2}(n) = \underline{\theta}(n)'\underline{y}(n-1) \tag{8.72b}$$

where

$$\underline{\theta}(n) = [a(n) \quad b(n) \quad c(n)]' \tag{8.74}$$

and

$$\underline{y}(n-1) = [\Delta F_{ETCO_2}(n-1)\ \Delta \dot{V}_E(n-1)\ \Delta F_{ICO_2}(n-1)]' \tag{8.75}$$

Thus, Equation (8.73) can be rewritten as

$$J(n) = \sum_{i=0}^{n} \lambda^{n-i}\left(\Delta F_{ETCO_2}(n) - \underline{\theta}(n)'\underline{y}(n-1)\right)^2 \tag{8.76}$$

We deduce the optimal value of $\underline{\theta}(n)$ that minimizes $J(n)$ by differentiating Equation (8.76) with respect to $\underline{\theta}(n)$ and setting the result equal to the null vector:

$$\frac{\partial J(n)}{\partial \underline{\theta}(n)} = -2\sum_{i=0}^{n} \lambda^{n-i}\left(\Delta F_{ETCO_2}(i) - \underline{\theta}(n)'\underline{y}(i-1)\right)\underline{y}(i-1)' = 0 \tag{8.77}$$

Rearranging terms in Equation (8.77), we obtain the following expression for the parameter vector:

$$\underline{\theta}(n) = \mathbf{R}(n)^{-1}\underline{r}(n) \tag{8.78}$$

where

$$\mathbf{R}(n) = \sum_{i=0}^{n} \lambda^{n-i} \underline{\mathbf{y}}(i-1)\underline{\mathbf{y}}(i-1)' \tag{8.79a}$$

and

$$\underline{r}(n) = \sum_{i=0}^{n} \lambda^{n-1} \Delta F_{\mathrm{ETCO}_2}(i)\underline{\mathbf{y}}(i-1) \tag{8.80a}$$

Note that, by separating the last term from the rest of the summation on the right-hand side, we can rewrite Equation (8.79a) in recursive form:

$$\mathbf{R}(n) = \underline{\mathbf{y}}(n-1)\underline{\mathbf{y}}(n-1)' + \lambda \mathbf{R}(n-1) \tag{8.79b}$$

Similarly, $r(n)$ in Equation (8.80a) can also be expressed in recursive form:

$$\underline{r}(n) = \Delta F_{\mathrm{ETCO}_2}(n)\underline{\mathbf{y}}(n-1) + \lambda \underline{r}(n-1) \tag{8.80b}$$

If we define the matrix $\mathbf{P}(n)$ to be the inverse of $\mathbf{R}(n)$:

$$\mathbf{P}(n) \equiv \mathbf{R}(n)^{-1} \tag{8.81}$$

then, using the matrix inversion lemma, it can be shown (through a somewhat complicated proof) that $\mathbf{P}(n)$ can be expressed in the recursive form:

$$\mathbf{P}(n) = \frac{1}{\lambda}\left(\mathbf{P}(n-1) - \frac{\mathbf{P}(n-1)\underline{y}(n-1)\underline{y}(n-1)'\mathbf{P}(n-1)}{\lambda + \underline{y}(n-1)'\mathbf{P}(n-1)\underline{y}(n-1)}\right) \tag{8.82}$$

Using Equation (8.80b) and Equation (8.82) in Equation (8.78), we obtain, after some algebraic manipulation, the following parameter update equation:

$$\underline{\theta}(n) = \underline{\theta}(n-1) + \underline{\mathbf{K}}(n)e(n) \tag{8.83}$$

where

$$\underline{K}(n) = \frac{P(n-1)\underline{y}(n-1)}{\lambda + \underline{y}(n-1)'P(n-1)\underline{y}(n-1)} \tag{8.84}$$

$\underline{K}(n)$ is a gain vector that determines the relative contribution of the prediction error, $e(n)$, to the estimate of the parameter vector $\underline{\theta}(n)$. $\underline{K}(n)$ depends on the $\mathbf{P}(n-1)$, which turns out to be the *parameter error covariance matrix* (see Section 7.3.2).

***8.5.2.3. Adaptive Control Law.*** Having estimated the most current values of the plant model parameters, the next task in each time step (breath) would be to determine the optimal value of $\Delta F_{\mathrm{ICO}_2}$ in the current breath (i.e., $\Delta F_{\mathrm{ICO}_2}(n-1)$) that would minimize the predicted $\Delta F_{\mathrm{ETCO}_2}$ at the end of the expiration phase of the current breath (i.e., $\Delta F_{\mathrm{ETCO}_2}(n)$). However, the criterion function to be minimized, in this case, was selected by Modarreszadeh et al. (1993) to be

$$I(n) = \left[\alpha\, \Delta F^{*}_{\mathrm{ETCO}_2}(n)\right]^2 + \left[\beta\, \Delta F_{\mathrm{ICO}_2}(n-1)\right]^2 \tag{8.85}$$

By including the term with $\Delta F_{\mathrm{ICO}_2}(n-1)$ in Equation (8.85), the fluctuations in inhaled $CO_2$ concentration are minimized along with those in alveolar $CO_2$. This allows for a solution that does not lead to minimal $\Delta F_{\mathrm{ETCO}_2}$ at the "expense" of employing large $\Delta F_{\mathrm{ICO}_2}$. This is

important from a practical point of view, since high values of $F_{ICO_2}$ can be a source of unpleasant sensation to the subject. The relative contributions of $\Delta F_{ETCO_2}$ and $\Delta F_{ICO_2}$ to the criterion function are determined by the weights $\alpha$ and $\beta$. Based on their experience, the authors chose values of 1 for $\alpha$ and 0.5 for $\beta$.

To determine the "optimal" $\Delta F_{ICO_2}(n-1)$, Equation (8.72a) is substituted into Equation (8.85) and this is differentiated with respect to $\Delta F_{ICO_2}(n-1)$. The result of the differentiation is set equal to zero. After rearranging terms, we obtain

$$\Delta F_{ICO_2}(n-1) = \frac{-\alpha^2 c(n-1)}{\alpha^2 c(n-1)^2 + \beta^2}\left[a(n-1)\,\Delta F_{ETCO_2}(n-1) + b(n-1)\,\Delta \dot{V}_E(n-1)\right] \tag{8.86}$$

In Equation (8.86), note that the plant parameter estimates from the previous breath (i.e., $a(n-1)$, $b(n-1)$, and $c(n-1)$) are used since, from Equations (8.83) and (8.84), the

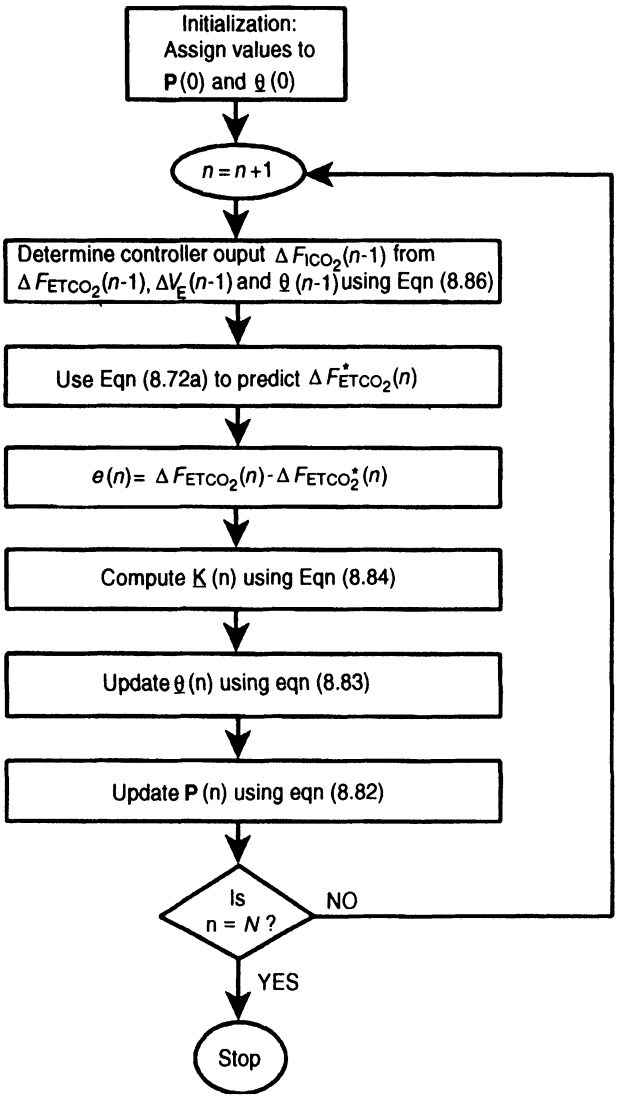


**Figure 8.10** Flowchart of adaptive control algorithm.

parameter estimates from the current breath (i.e., $a(n)$, $b(n)$, and $c(n)$) are determined in part by $\Delta F_{ICO_2}(n-1)$.

The overall algorithm for the adaptive control scheme is displayed in the form of a flowchart in Figure 8.10. When the algorithm is initiated from starting conditions ($n = 0$), it is useful to employ initial values for the plant parameters that are not too far from their "true" values. For this reason, Modarreszadeh et al. estimated these values beforehand by measuring the subjects' responses to a dynamic $CO_2$ stimulus that was altered in pseudorandom binary fashion (see Section 7.5.2.1). The average values of $a$, $b$, and $c$ in eight subjects were found to be 0.66, −0.02, and 0.69, respectively. The value for $b$ assumes that ventilation is measured in L $min^{-1}$ and $F_{ETCO_2}$ is expressed as a percentage. A starting value for the parameter error covariance matrix, **P**, is also required. A common procedure is to set **P**(0) equal to the identity matrix scaled by a factor of 100.

***8.5.2.4. Performance of the Adaptive Controller.*** Breath-by-breath measurements of $F_{ETCO_2}$ in a normal subject during spontaneous breathing are shown in Figure 8.11a. These can be compared to the corresponding measurements of $F_{ETCO_2}$ in the same subject during adaptive buffering of the end-tidal $CO_2$ fluctuations, shown in Figure 8.11b. It is clear that the adaptive controller produced a significant reduction of the fluctuations in $F_{ETCO_2}$, particularly in the lower-frequency region. It would have been possible reduce $\Delta F_{ETCO_2}$ further by setting $\beta$ in the criterion function I(n) to zero. But this would be achieved at the expense of incurring larger fluctuations in $F_{ICO_2}$.

The properties of this adaptive control scheme can be studied further by executing the MATLAB script file "`acs_CO2.m`" included with this book. However, instead of obtaining

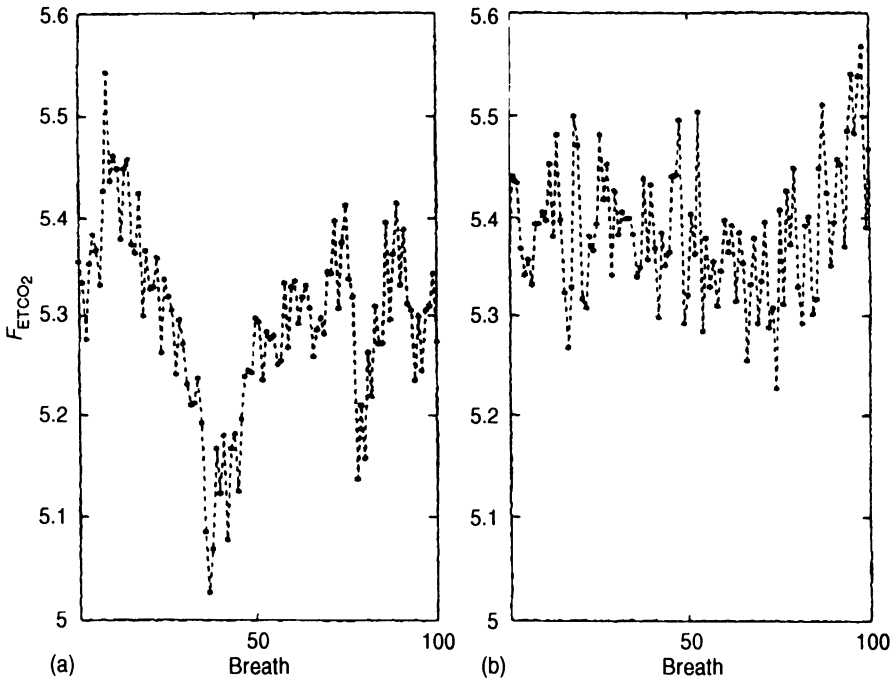


**Figure 8.11** (a) Breath-by-breath measurements of $F_{ETCO_2}$ in an adult human, showing considerable spontaneous variability. (b) $F_{ETCO_2}$ measurements in the same subject during application of the adaptive buffering scheme (Reproduced from Modarreszadeh et al., 1993)

measurements for a real human subject, a simple dynamic simulation of the chemoreflex control system is used to generate "data" and to interact with the adaptive controller. The fluctuations in $\dot{V}_E$, $F_{ICO_2}$, and $F_{ETCO_2}$ are assumed to occur around their corresponding mean levels.

## BIBLIOGRAPHY


Akay, M. *Biomedical Signal Processing*. Academic Press, New York, 1994.

Astrom, K.J., and B. Wittenmark. *Adaptive Control*. Addison-Wesley, Reading, MA, 1989.

Clarke, D.W., and P.J. Gawthrop. Self-tuning controller. *Proc. IEEE* **122**: 922–934, 1975.

Elsgolc, L.E. *Calculus of Variations*. Addison-Wesley, Reading, MA, 1962.

Fischer, U., W. Schenk, E. Salzsieder, G. Albrecht, P. Abel, and E.J. Freyse. Does physiological blood glucose control require an adaptive control strategy. *IEEE Trans. Biomed. Eng.* **BME-34**: 575–582, 1987.

Harris, C.J., and S.A. Billings (eds.). *Self-tuning and Adaptive Control: Theory and Applications*. Institute of Electrical Engineers (U.K.), London, 1981.

Katona, P.G. On-line control of physiological variables and clinical therapy. *CRC Rev. Biomed. Eng.* **8**: 281–310, 1982.

Livnat, A., and S.M. Yamashiro. Optimal control evaluation of left ventricular systolic dynamics. *Am. J. Physiol.* **240**: R370–R383, 1981.

Martin, J.F., A.M. Schneider, and N.T. Smith. Multiple-model adaptive control of blood pressure using sodium nitroprusside. *IEEE Trans. Biomed. Eng.* **BME-34**: 603–611, 1987.

Mead, J. Control of respiratory frequency. *J. Appl. Physiol.* **15**: 325–336, 1960.

Milsum, J.H. Optimization aspects in biological control theory. In: *Advances in Biomedical Engineering and Medical Physics*, Vol. 1 (edited by S.N. Levine). Wiley Interscience, New York, 1968; pp. 243–278.

Modarreszadeh, M., K.S. Kump, H.J. Chizeck, D.W. Hudgel, and E.N. Bruce. Adaptive buffering of breath-by-breath variations of end-tidal $CO_2$ in humans. *J. Appl. Physiol.* **75**: 2003–2012, 1993.

Olkkola, K.T., and H. Schwilden. Adaptive closed-loop feedback control of vecuronium-induced neuromuscular relaxation. *Eur. J. Anaesth.* **8**: 7, 1991.

Orfanidis, S. *Optimum Signal Processing*. McGraw-Hill, New York, 1988.

Otis, A.B., W.O. Fenn, and H. Rahn. Mechanics of breathing in man. *J. Appl. Physiol.* **2**: 592–607, 1950.

Poon, C.-S. Ventilatory control in hypercapnia and exercise: optimization hypothesis. *J. Appl. Physiol.* **62**: 2447–2459, 1987.

Rohrer, F. Physiologie der Atembewegung. In: A. Bethe et al. (Eds.), *Handbuch der normalen und pathologischen Physiologie*. Springer, Berlin, 1925. Vol. 2, p. 70–127.

Ruttimann, U.E., and W.S. Yamamoto. Respiratory airflow patterns that satisfy power and force criteria of optimality. *Ann. Biomed. Eng.* **1**: 146–159, 1972.

Yamashiro, S.M., J.A. Daubenspeck, and F.M. Bennett. Optimal regulation of left ventricular ejection pattern. *Appl. Math. Comp.* **5**: 41–54, 1979.

Yamashiro, S.M., and F.S. Grodins. Optimal regulation of respiratory airflow. *J. Appl. Physiol.* **30**: 597–602, 1971.

## PROBLEMS

**P8.1.** The rate at which energy is expended in walking, as measured by oxygen consumption, has been found to take the form:

$$P = 0.267V^2 + 2160$$

where the velocity of walking, $V$, is given in meters per minute, and $P$ is in calories per minute. Determine the value of the walking speed that would minimize the *energy expended per unit distance*. Also, determine the power consumption rate at this optimal speed.

**P8.2.** In the Otis model discussed in Section 8.2, derive an expression for the optimal respiratory frequency, $f_{opt}$, that would minimize the work-rate of breathing if the nonlinear resistance term in Equation (8.12) were to be omitted. $f_{opt}$ should be expressed in terms of the lung mechanical parameters $K$ and $K'$, as well as the alveolar ventilation $\dot{V}_A$ and dead space volume $V_D$. Determine the optimal breathing frequency (in breaths $min^{-1}$) when $K = 8.5$ (cm $H_2O$) $L^{-1}$, $K' = 0.0583$ (cm $H_2O$) min $L^{-1}$, $\dot{V}_A = 6$ L $min^{-1}$, and $V_D = 0.2$ L.

**P8.3.** On the basis of minimization of work-rate, the Yamashiro and Grodins (1971) model predicted a rectangular inspiratory airflow pattern that is not generally observed in resting humans. This suggested to them that, during resting conditions, the respiratory system may be minimizing a different criterion function. They proposed this other criterion function to be the mean squared acceleration, *MSA*, defined as

$$MSA \equiv \frac{1}{T}\int_0^T \left(\frac{d\dot{V}}{dt}\right)^2 dt$$

where $T = 1/f$ and $f$ = respiratory frequency. Using the Lagrange multiplier method, show that the Fourier coefficients of the optimal airflow waveform that minimizes *MSA* (given the constraint of constant $\dot{V}_A$ and $V_D$) are given by

$$a_{2i-1} = \frac{384(fV_D + \dot{V}_A)}{4\pi^3(2i-1)^3}$$

To arrive at the above result, you will need to use the following equality:

$$\sum_{i=1}^{\infty} \frac{1}{(2i-1)^4} = \frac{\pi^4}{96}$$

Plot one cycle of the optimal airflow waveform, using only the first four harmonics of the Fourier series. Assume $\dot{V}_A = 6$ L $min^{-1}$ and $V_D = 0.2$ L.

**P8.4.** Use the method of calculus of variations to derive an expression for the optimal respiratory frequency in Otis's model, assuming the nonlinear resistance term can be neglected. The constraint to be imposed is that of constant $\dot{V}_A$ and $V_D$. You should arrive at the same result as in Problem P8.2.

**P8.5.** Using the MATLAB script file "`OptLVEF.m`," determine the optimal value of systolic duration and the optimal left ventricular output pattern that would minimize the energy dissipated per cardiac cycle in a typical human. Determine also the power consumption (in calories per second) of this optimal flow pattern. As well, determine the optimal time-course of left ventricular pressure over a cardiac cycle. Assume the following representative parameter values for an adult human: stroke volume = 80 ml, heart rate = 72 beats $min^{-1}$, $R_P = 1.2$ mm Hg s $ml^{-1}$, $R_C = 0.01$ mm Hg s $ml^{-1}$, $C_a = 2.3$ ml mm $Hg^{-1}$, $q_0 = 80$ ml $s^{-1}$.

**P8.6.** In mild to moderate exercise, there is an increase in ventilation ($\dot{V}_E$) that is approximately proportional to the increase in metabolic rate. Yet, in humans, arterial $P_{CO_2}$ ($P_{aCO_2}$) remains relatively constant at its resting level of ~40 mm Hg. This observation has sparked many theories about the underlying mechanism for this "exercise hyperpnea," since the increase in ventilation apparently is not due to chemoreflex mediation (for otherwise, $P_{aCO_2}$ should increase). Poon (1987) has proposed that the isocapnic exercise response can be accounted for if one postulates that $\dot{V}_E$ is governed by an optimization policy of the respiratory controller. He suggested that $\dot{V}_E$ is selected so as to minimize a criterion function that includes both the chemical and mechanical "cost" of breathing:

$$J = (\alpha P_{aCO_2} - \beta)^2 + 2\ln(\dot{V}_E)$$

while satisfying the constraint imposed by gas exchange considerations, i.e.,

$$P_{aCO_2} = \frac{863\dot{V}_{CO_2}}{\dot{V}_E\left(1 - \frac{V_D}{V_T}\right)}$$

where $V_D/V_T$, the ratio of dead space to tidal volume, is assumed constant, and $\dot{V}_{CO_2}$ is the metabolic production rate for $CO_2$ (assumed to be proportional to exercise intensity). By performing a constrained minimization, show that this model predicts a level of $P_{aCO_2}$ that is independent of $\dot{V}_{CO_2}$. Assuming model parameters of $\alpha = 0.1$ mm Hg$^{-1}$, $\beta =$ 37 mm Hg, and $V_D/V_T = 0.2$, plot $J$ versus $\dot{V}_E$ under resting ($\dot{V}_{CO_2} = 0.2$ L min$^{-1}$) and exercise ($\dot{V}_{CO_2} = 1$ L min$^{-1}$) conditions, and determine the optimal $\dot{V}_E$ and minimum $J$ in each case.

**P8.7.** Using the MATLAB script file "`acs_CO2.m`," determine how the ratio of the variance (= standard deviation$^2$) of the fluctuations in $F_{ETCO_2}$ during adaptive buffering to the corresponding variance of $F_{ETCO_2}$ during spontaneous breathing (no buffering) will change as the weighting factor $\beta$ for $F_{ICO_2}$ in the control law is changed from 0 to 1; plot this relative variance as a function of $\beta$. Determine also how these changes in $\beta$ would affect the fluctuations in $F_{ICO_2}$. Use increments of 0.1 in $\beta$.